

# Analysis in the Effect of Co-phase Traction Railway HPQC Coupled Impedance on Its Compensation Capability and Impedance-Mapping Design Technique Based on Required Compensation Capability for Reduction in Operation Voltage

Keng-Weng Lao, *Student Member, IEEE*, Man-Chung Wong, *Senior Member, IEEE*,  
NingYi Dai, *Senior Member, IEEE*, Chi-Seng Lam, *Senior Member, IEEE*,  
Chi-Kong Wong, *Member, IEEE*, and Lei Wang

**Abstract**—Railway hybrid power quality conditioner (HPQC) is one of the newly proposed devices for power quality compensation in co-phase high-speed traction power supply for its benefit in reduction of operation voltage over conventional railway power quality conditioner (RPC). However, initial railway HPQC design is developed based on minimum operation voltage at predefined fixed rated load. This may not be applicable in practical condition when load varies. In order to solve this problem, a railway HPQC design with increased operation voltage has been investigated to enhance the compensation capability. Nevertheless, the compensation capability is even larger than that required during load variations such that the operation voltage is higher than it actually requires. A lower operation voltage can actually be used to provide required compensation capability when the coupled impedance is different from the designed rated one. In this paper, the effect of coupled impedance on the compensation capability in co-phase railway HPQC is being analyzed. An impedance-mapping design technique based on required compensation capability is then proposed based on the analysis. The proposed method is advantageous for lower operation voltage and smaller capacitance value. The effectiveness of impedance-mapping technique is verified via simulation and experimental results.

Manuscript received March 27, 2016; accepted May 18, 2016. Date of publication June 1, 2016; date of current version January 20, 2017. This work was supported by the Science and Technology Development Fund under Project 015/2008/A1, the Macao SAR Government, and the University of Macau Research Committee under Project UL015/08-Y2/EEE/WMC01/FST and Project MYRG2015-00009-FST. Recommended for publication by Associate Editor T. Lebey.

K.-W. Lao, N. Dai, C.-K. Wong, and L. Wang are with the Department of Electrical and Computer Engineering, Faculty of Science and Technology, University of Macau, Macao 999078, China. (e-mail: yb17424@umac.mo; nydai@umac.mo; ckwong@umac.mo).

M.-C. Wong is with the Department of Electrical and Computer Engineering, Faculty of Science and Technology and also with the State Key Laboratory of Analog and Mixed Signal VLSI, University of Macau, Macao, China (e-mail: mcwong@umac.mo).

C.-S. Lam is with the State Key Laboratory of Analog and Mixed Signal VLSI, University of Macau, Macao, China (e-mail: cslam@umac.mo).

L. Wang is with the Department of Electrical and Computer Engineering, University of Macau, Macao, China. (e-mail: jordanwanglei@gmail.com).

Color versions of one or more of the figures in this paper are available online at <http://ieeexplore.ieee.org>.

Digital Object Identifier 10.1109/TPEL.2016.2575446

**Index Terms**—Co-phase traction power supply, high-speed railway, impedance mapping, power quality, railway hybrid power quality conditioner (HPQC).

## I. INTRODUCTION

POWER quality compensation is of essential importance in traction power supply. Existence of power quality problems in critical power systems can threaten system stability and may damage devices or even cause system failure, which may result in massive economic losses. Thus, it is merely important to get rid of traction power quality problems [1].

Traction power supply without proper compensation usually suffers from different power quality problems. Major traction power quality problems are mainly system unbalance, reactive power, and harmonics [2]–[4]. Concerning these power quality problems, IEEE has developed standards for its tolerances in different power systems [5]. Various power quality compensation devices have been proposed for traction power. Conventionally, compensators such as shunt capacitive bank, passive filters, and static var compensator (SVC) are used [6]–[8]. For instance, the usage of shunt capacitor for railway locomotive power was presented in 1948 in [8]. However, their dynamic performance is poor. Compensators based on active components are therefore proposed [8], [9]. They have better dynamic performance and is widely used. In 2000, the usage of thyristor-switched capacitor for traction power is reported in [10].

Most high-speed railway locomotives are electrified with 25 kV ac power [14]. In order to overcome the locomotive limitation problems of existing high-speed traction power, the co-phase traction power is being introduced and studied in 2006 [15]. Shown in Fig. 1 are the circuit schematics of conventional and newly proposed co-phase traction power, respectively. Power to locomotives is obtained via three-phase source grid through substation transformer.

In conventional traction power system, locomotive power is obtained via two different phase outputs such that neutral sections are required to avoid risk of phase mixing. Locomo-

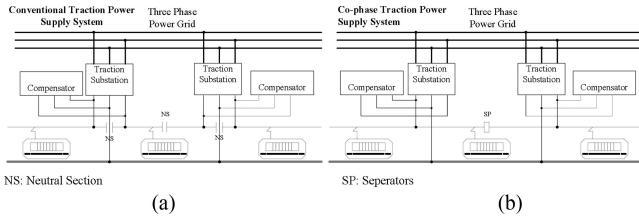


Fig. 1. Circuit schematics of (a) conventional traction power supply system; (b) co-phase traction power supply system.

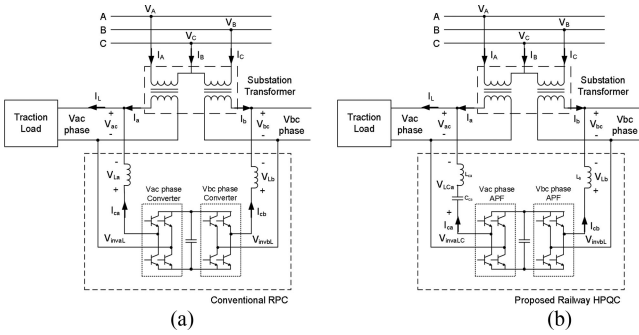


Fig. 2. Detailed circuit schematics of (a) co-phase traction power supply system with conventional RPC; (b) co-phase traction power supply system with proposed railway HPQC.

tives lose power when passing through neutral sections and make the structure not suitable for high-speed railway. On the other hand, in co-phase traction, locomotive power is obtained from one single-phase only and the quantity of isolation components can thus be effectively reduced [16]–[18]. The structure is therefore suitable for high-speed railway. It is worth noticed that the world's first co-phase traction device has already been installed and put into operation at the MeiShan Traction Substation of the Chengdu-Kunming Railway in China in 2010 [19], [20].

In co-phase traction power, railway power quality conditioner (RPC) is used to provide power quality compensation in co-phase traction power [11]–[13]. A typical circuit of co-phase traction power with RPC is shown in Fig. 2(a). The RPC is basically composed of a back-to-back converter with a common dc link, and is connected across the two substation single-phase outputs to provide compensation for three-phase power grid. However, with inductive coupled impedance, the RPC operation voltage must be higher than point of common coupling (PCC) voltage peak value and induces high cost.

Based on the consideration above, the co-phase traction power supply with railway hybrid power quality conditioner (HPQC) shown in Fig. 2(b) is first proposed by our research group in 2012 [21]. Different from conventional RPC, a hybrid LC-branch structure is adopted in the converter to reduce the compensator system and device rating. Notice that hybrid structure is adopted in  $V_{ac}$  phase converter only since operation voltage reduction can be achieved only when the converter is used to output power ( $V_{bc}$  phase converter is used to absorb power). The detailed railway HPQC structure and control algorithm can be found in [22] and [23]. A railway HPQC based on minimum operation voltage requirement at rated load was proposed in [24], [25]. However, the minimum operation voltage is only valid at rated load and

may not be applicable when load varies. Although the operation voltage can be minimized at rated load, the compensation capability is minimized, the operation voltage thus needs to be enhanced to a high value and excessive compensation capability is resulted [26]. This is due to that the coupled impedance is determined based on rated load only. It is obvious that the coupled impedance will affect the compensation capability under the same operation voltage level. When the coupled impedance is different from rated one, the operation voltage requirement may be reduced while providing similar performance within the load condition range (range of compensation capability) and can reduce initial cost.

Railway HPQC in co-phase traction power supply is first proposed by our research group and so far the following have been investigated:

- 1) adoption of hybrid structure in co-phase railway HPQC [21];
- 2) derivation of control algorithm in railway HPQC [22], [23];
- 3) analysis of railway HPQC operation and minimum operation voltage based on fixed rated load [24], [25];
- 4) investigation of the relationship between railway HPQC operation voltage and compensation capability for providing satisfactory performance within load variations [26].

Based on the considerations of high operation voltage during load variations mentioned earlier, in this paper, the effect of coupled impedance on the compensation capability of railway HPQC in co-phase traction power is being analyzed. Based on the analysis, a novel impedance mapping technique is proposed for reduction of operation voltage and coupled capacitance in railway HPQC. The core idea is to map the coupled impedance with the required compensation capability range.

In Section I, a brief introduction of research background motivation of investigating the effect of coupled impedance on co-phase traction railway HPQC compensation capability and proposing impedance-mapping railway HPQC is presented. In Section II, the system control and model of railway HPQC is provided for the analysis in this paper. The concept of compensation range to evaluate the compensation capability and the effect of railway HPQC coupled impedance on compensation capability is explored in Section III. In Section IV, the impedance-mapping design technique in railway HPQC by mapping the coupled impedance with required compensation capability is proposed. Furthermore, the effectiveness of operation voltage and coupled capacitance reduction using proposed technique is explored. The detailed design procedure of railway HPQC using proposed impedance-mapping technique is presented in Section V. A railway HPQC using proposed impedance-mapping technique is then designed based on practical traction power data obtained from China WuQing substation [27]. PSCAD simulations are performed and shown in Section VI. A laboratory scale hardware prototype is also constructed. The experimental results obtained are presented to show the effectiveness of proposed impedance-mapping design technique for reduction of operation voltage requirement and coupled capacitance without affecting the performance within required compensation capability are shown in Section VII. Finally, a conclusion is given in Section VIII.

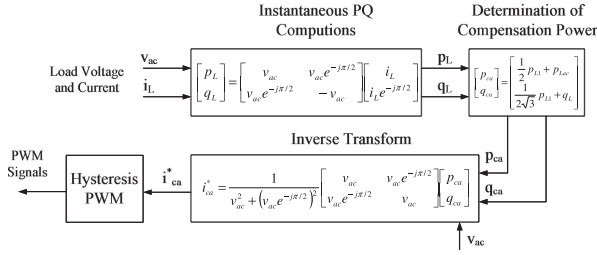


Fig. 3. System control block diagram of railway HPQC in co-phase traction power quality compensation.

## II. SYSTEM MODEL AND CONTROL OF RAILWAY HPQC

In co-phase traction power, railway HPQC compensation power is injected to the secondary side of traction power substation transformer in order to provide power compensation in the primary grid. Details about railway HPQC modeling and control can be found in [21] and [23]. The system model and control of railway HPQC for analysis are introduced later.

### A. System Model of Co-phase Power with Railway HPQC

As observed from Fig. 2, railway HPQC is composed of a  $V_{ac}$  phase and a  $V_{bc}$  phase converters connected back-to-back with a common dc link. The compensation current from the two converters is defined as  $I_{ca}$  and  $I_{cb}$ , respectively, with the active and reactive power output defined as  $p_{ca}$ ,  $q_{ca}$  and  $p_{cb}$ ,  $q_{cb}$ . The angle between voltage  $V_{ac}$  and compensation current  $I_{ca}$  is defined as  $\theta_{ca}$ . It is also assumed that the traction load is drawing load current  $I_L$  from the system, with  $p_L$  and  $q_L$  as load active and reactive power.

### B. System Control of Railway HPQC

Under ideal compensation, the primary source power grid should be free of power quality problems (unity power factor (PF), zero unbalance, and harmonics). The required compensation power output by railway HPQC can then be derived based on the compensation requirements. Detailed derivation procedures are presented in [22] and [23]. The required compensation power, which is also the core algorithm, is shown in (1). It can be observed that power quality compensation in co-phase traction is accomplished by the transfer of active and reactive power.

The control block diagram of the railway HPQC for co-phase traction power supply is given in Fig. 3. It is mainly used to generate the compensation current reference  $i_{ca}^*$

$$\begin{bmatrix} p_{ca} \\ q_{ca} \\ p_{cb} \\ q_{cb} \end{bmatrix} = \begin{bmatrix} \frac{1}{2}\bar{p}_L + \bar{p}_L \\ \frac{1}{2\sqrt{3}}\bar{p}_L + q_L \\ -\frac{1}{2}\bar{p}_L \\ -\frac{1}{2\sqrt{3}}\bar{p}_L \end{bmatrix}. \quad (1)$$

According to (1), the negative sign of  $p_{cb}$  and  $q_{cb}$  indicate that during compensation, active power and reactive power are absorbed from the system to the  $V_{bc}$  phase converter. A positive voltage drop across the coupled inductance is thus resulted and

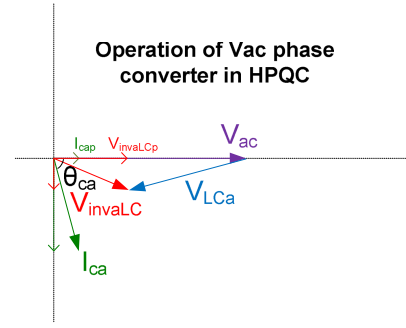


Fig. 4. Phasor diagram of  $V_{ac}$  phase converter operation in railway HPQC compensation for co-phase high-speed traction power supply.

makes it possible that the  $V_{bc}$  phase converter operation voltage requirement can be less than the  $V_{bc}$  phase voltage. On the other hand, when the coupled impedance is capacitive, the  $V_{bc}$  phase converter operation voltage requirement will be higher than  $V_{bc}$  phase voltage and the railway HPQC operation voltage requirement will be high, which degrades the advantages of railway HPQC. Therefore, asymmetric coupled impedance topology is adopted in railway HPQC. More detailed information about  $V_{bc}$  phase converter design was mentioned in [24] and [25]. It is shown through the results that the dc-link operation voltage of railway HPQC is dominated by  $V_{ac}$  phase converter design. Therefore,  $V_{bc}$  phase converter is not discussed in this paper.

Finally, after getting  $i_{ca}^*$ , this current can be injected into the system through  $V_{ac}$  phase converter by hysteresis pulsewidth modulation (PWM) in linear operation region given in [28]. In the following section,  $I_{ca} = i_{ca}^*$  is assumed for simplicity in the following sections as it does not affect the theoretical deduction in this paper since the focus of this paper is system capacity.

In railway HPQC, the power converters used are voltage source converters. With PWM-controlled switches, the ac voltage is chopped at inverter output, while the output compensation current is allowed to be controlled in different directions. Therefore, the hybrid  $LC$ -coupled structure can somehow act as a low-pass filter to filter the chopped waveforms and reduce the harmonics in the output compensation current.

## III. CONCEPT OF COMPENSATION RANGE TO EVALUATE COMPENSATION CAPABILITY IN RAILWAY HPQC AND EFFECT OF RAILWAY HPQC COUPLED IMPEDANCE ON COMPENSATION CAPABILITY

### A. Concept of Compensation Range to Evaluate Compensation Capability

A phasor diagram showing the operation of  $V_{ac}$  phase converter in railway HPQC during compensation is given in Fig. 4.

The relationship can be further investigated mathematically, as shown in (2)

$$\begin{aligned} |V_{invaLC}| &= \sqrt{V_{invaLCp}^2 + V_{invaLCq}^2} \\ &= \sqrt{(V_{ac} - |I_{caq}| |X_{LCa}|)^2 + (|I_{cap}| |X_{LCa}|)^2} \end{aligned} \quad (2)$$

where

$$I_{cap} = I_{ca} \cos \theta_{ca} \quad I_{caq} = I_{ca} \sin \theta_{ca}$$

$$\theta_{ca} = \tan^{-1} \left( \frac{\frac{1}{\sqrt{3}} (\text{PFL}) + \sin (\cos^{-1} (\text{PFL}))}{\frac{1}{2} (\text{PFL})} \right)$$

where PFL is the displacement load PF.

During load variations, the load capacity and PF may change. Two parameters  $r$ ,  $h_s$ , and  $h_c$  are added to represent variations. It is supposed that railway HPQC is designed according to rated values, the load capacity is changed to  $r$  times of rated value. Referring to (1), it can be deduced that the compensation current  $I_{ca}$  is changed to  $r$  times of rated values, represented as  $r I_{ca}$ . The parameter  $r$  can therefore be used to define load and compensation range. The compensation angle  $\theta_{ca}$  is changed such that the value of  $\cos(\theta_{ca})$  and  $\sin(\theta_{ca})$  is changed to  $h_c \cos(\theta_{ca, \text{rated}})$  and  $h_s \sin(\theta_{ca, \text{rated}})$ , respectively. These variations can be represented by the ratio of compensation power to rated ones, as shown in (3)

$$\begin{cases} \frac{p_{ca}}{p_{ca, \text{rated}}} = \frac{V_{ac} \cdot r \cdot (I_{ca, \text{rated}}) \cdot h_c (\cos \theta_{ca, \text{rated}})}{V_{ac} \cdot (I_{ca, \text{rated}}) \cdot (\cos \theta_{ca, \text{rated}})} = r \cdot h_c \\ \frac{q_{ca}}{q_{ca, \text{rated}}} = \frac{V_{ac} \cdot r \cdot (I_{ca, \text{rated}}) \cdot h_s (\sin \theta_{ca, \text{rated}})}{V_{ac} \cdot (I_{ca, \text{rated}}) \cdot (\sin \theta_{ca, \text{rated}})} = r \cdot h_s \end{cases} \quad (3)$$

By substituting (3) into (2), the compensation current  $I_{cap}$  and  $I_{caq}$  is changed, as given in (4)

$$\begin{cases} I_{cap} = r (I_{ca, \text{rated}}) \cdot h_c (\cos \theta_{ca, \text{rated}}) \\ I_{caq} = r (I_{ca, \text{rated}}) \cdot h_s (\sin \theta_{ca, \text{rated}}) \end{cases} \quad (4)$$

A graph showing the variation of  $h_s$  value with load PF under different design rated  $P_{FLr}$  is plotted in Fig. 5 according to (3). Notice that the railway HPQC is usually designed based on rated value and that the rated load PF is denoted as  $P_{FLr}$  in the figure. The rated values 0.7, 0.8, 0.85, and 0.9 are chosen since locomotive load PF usually ranges from 0.8 to 0.9. This is useful for later analysis.

By substituting (4) into (2), the expression for railway HPQC operation voltage shown in (5) shown at the bottom of the page.

In order to eliminate the effect of rated parameters during analysis, it is further assumed that the  $V_{ac}$  phase-coupled impedance is expressed as a function of rated voltage and compensation current, as shown in (6)

$$X_{LCa} = m_{LCa} \cdot \left| \frac{V_{ac}}{I_{ca, \text{rated}}} \right|. \quad (6)$$

The value of coupled impedance ratio  $m_{LCa}$  is therefore directly proportional to the coupled impedance  $X_{LCa}$ . In other words, a lower value of  $m_{LCa}$  indicates smaller coupled impedance  $X_{LCa}$ . A simplified expression for operation voltage may then be obtained by substituting (6) back into (5), as shown in (7). The expression is also divided by voltage  $V_{ac}$  in

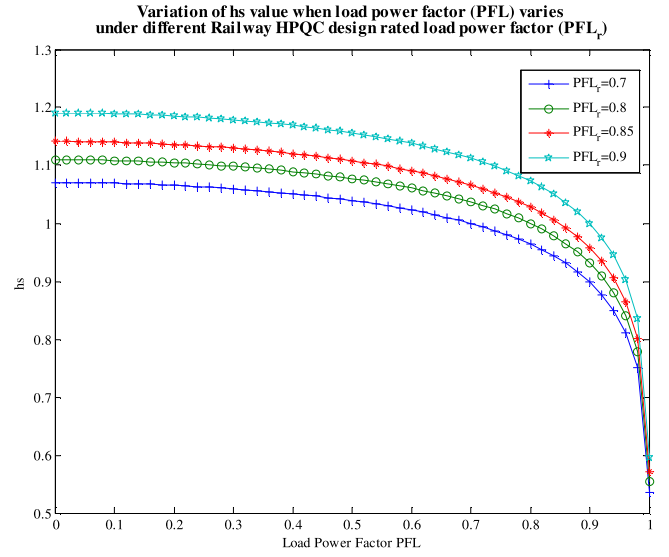


Fig. 5. MATLAB plot showing the variation of  $h_s$  values with load PF (under different design rated  $P_{FLr}$ ).

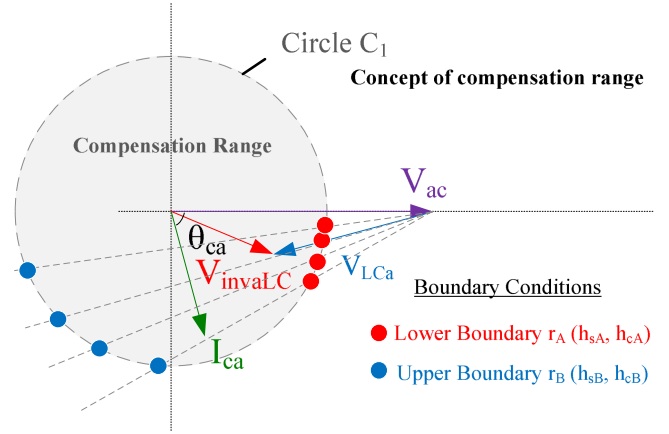


Fig. 6. Phasor diagram showing the concept of compensation range in railway HPQC operation.

order to determine the railway HPQC operation voltage rating equation (7) is shown bottom of the page.

In (7), the parameters  $r$ ,  $h_s$ , and  $h_c$  define load variations; with the parameter  $\theta_{ca, \text{rated}}$  as a constant rated value, it can be observed that the range of loadings, which can be compensated is determined by the operation voltage rating  $k_{invaLC}$  and coupled impedance ratio  $m_{LCa}$ .

A phasor diagram showing the concept of compensation range is shown in Fig. 6. The shaded area represents the compensation range and can be defined using the expression in (8) equation (8) is shown bottom of the page.

Notice that the component  $V_{LCa}$  represents the voltage across the coupled impedance  $X_{LCa}$  and is determined by (9)

$$V_{LCa} = \vec{I}_{ca} \cdot X_{LCa}. \quad (9)$$

$$|V_{invaLC}| = \sqrt{(V_{ac} - |r (I_{ca, \text{rated}}) \cdot h_s (\sin \theta_{ca, \text{rated}})| |X_{LCa}|)^2 + (|r (I_{ca, \text{rated}}) \cdot h_c (\cos \theta_{ca, \text{rated}})| |X_{LCa}|)^2} \quad (5)$$

The relationship between the parameters and the figure is briefly discussed as follows:

- 1) the railway HPQC operation voltage rating is defined by the radius of the circle  $C_1$ ;
- 2) as shown in (9), the coupled impedance  $X_{LCa}$  or its ratio  $m_{LCa}$  is directly proportional to the amplitude of vector  $V_{LCa}$ ;
- 3) similarly, the parameter  $r$  is directly proportional to the amplitude of vector  $V_{LCa}$ ;
- 4) the values of  $h_s$  and  $h_c$  actually define the components compensation active and reactive power, it therefore affects the direction of vector  $V_{LCa}$ .

It can be observed from Fig. 6 that as long as the vector  $V_{invaLC}$  is located inside the shaded area, satisfactory compensation performance can be provided by railway HPQC.

Referring to (4) again, as the load condition is different from rated one, for instance, when the values of  $r$ ,  $h_s$ , and  $h_c$  vary, the required railway HPQC compensation power and capability will also be different accordingly. Therefore, from now on, investigation of the compensation capability is achieved by investigating the compensation range parameters  $r$ ,  $h_s$ , and  $h_c$ .

#### B. Effect of Railway HPQC Coupled Impedance on Compensation Capability

Referring back to (8), it can be observed that under a certain operation voltage rating  $k_{invaLC}$ , as the coupled impedance ( $X_{LCa}$ ) is different, the compensation range/capability ( $r$ ,  $h_s$ ,  $h_c$ ) in which satisfactory compensation performance can be provided will also be different.

By further manipulation of (8), the expression in (10) can be obtained

$$\frac{h_s \sin \theta_{ca\_rated} - \sqrt{(h_s \cdot \sin \theta_{ca\_rated})^2 - 1 + (k_{invaLC})^2}}{m_{LCa}} \leq r \leq \frac{h_s \sin \theta_{ca\_rated} + \sqrt{(h_s \cdot \sin \theta_{ca\_rated})^2 - 1 + (k_{invaLC})^2}}{m_{LCa}}. \quad (10)$$

Locomotive load PF usually ranges from 0.8 to 0.9 [29]. Supposing that the locomotive load power is unchanged at PFL = 0.85 during variations such that  $h_c = h_s = 1$ , a graph is plotted using MATLAB according to (8) in Fig. 7. A MAT-

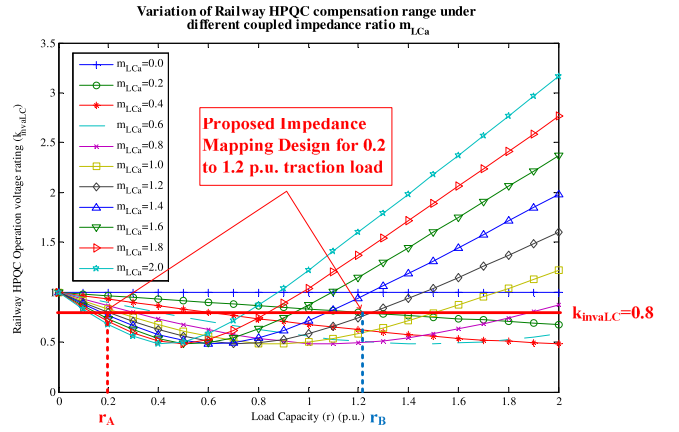


Fig. 7. MATLAB plot showing the variation of railway HPQC compensation range under different coupled impedance ratio  $m_{LCa}$  (Rated PFL = 0.85).

LAB plot is constructed according to (8) and (10) to show the variation of compensation range when the railway HPQC coupled impedance ratio  $m_{LCa}$  is different. This also shows the compensation capability.

The effect of railway HPQC coupled impedance on compensation capability in co-phase traction power may be investigated using (10) and Fig. 7. It can be observed that under a certain value of operation voltage rating ( $k_{invaLC}$ ), as the coupled impedance increases (the value of  $m_{LCa}$  increases), the range of loading capacity condition (value of  $r$ ) would be narrower, and the middle point of the compensation range would also vary. In other words, there is a specific combination coupled impedance ratio  $m_{LCa}$  and operation voltage rating  $k_{invaLC}$  that can provide satisfactory compensation for a desired range of load condition (capacity rating  $r_A$  to  $r_B$  and load PF  $h_{sA}$  and  $h_{sB}$ ) and compensation capability. This is also the core idea of proposed impedance-mapping design technique.

The proposed impedance-mapping design technique is beneficial for reduction of operation voltage and coupled capacitance. For example, assuming that traction load capacity ranges from 0.2 to 1.2 p.u. (as the case in WuQing substation in later analysis), as seen from Fig. 7, when railway HPQC operation voltage rating equals 0.85, the compensation range goes from around 0.2 to 1.2 when  $m_{LCa}$  equals 1.2. In [24], the railway HPQC is developed under minimum operation volt-

$$k_{invaLC} = \frac{|V_{invaLC}|}{V_{ac}} = \sqrt{(1 - |r \cdot h_s| \cdot m_{LCa} \cdot \sin \theta_{ca\_rated})^2 + (|r \cdot h_c| \cdot m_{LCa} \cdot \cos \theta_{ca\_rated})^2} \quad (7)$$

$$k_{invaLC} \geq \sqrt{(1 - |r \cdot h_s| \cdot m_{LCa} \cdot \sin \theta_{ca\_rated})^2 + (|r \cdot h_c| \cdot m_{LCa} \cdot \cos \theta_{ca\_rated})^2} \quad (8)$$

$$k_{invaLC} \geq \sqrt{(r \cdot m_{LCa})^2 - 2(r \cdot m_{LCa})(h_s \cdot \sin \theta_{ca\_rated}) + 1}$$

age requirement, and the value of  $m_{LCa}$  is 0.88 under similar condition (rated  $PF_L = 0.85$ ). Thus, the coupled impedance is larger when it is mapped with the compensation range. (A larger coupled impedance infers a lower coupled capacitance, and lower operation voltage rating. More about reduction in coupled capacitance and operation voltage will be discussed in next section).

#### IV. PROPOSED IMPEDANCE-MAPPING DESIGN TECHNIQUE IN RAILWAY HPQC FOR REDUCTION IN OPERATION VOLTAGE AND COUPLED CAPACITANCE

##### A. Proposed Impedance-Mapping Design Technique

By further manipulating the expression in (7), the coupled impedance ratio  $m_{LCa}$  can be expressed as a function in terms of railway HPQC operation voltage rating ( $k_{invaLC}$ ), and loading conditions range ( $r, h_s, h_c$ ), as shown in (11). The coupled impedance may therefore be determined based on required compensation range/capability ( $r, h_s$ )

$$m_{LCa} = \frac{(h_s)(\sin \theta_{ca, rated}) \pm \sqrt{(h_s)^2(\sin \theta_{ca, rated})^2 + (k_{invaLC})^2 - 1}}{r} \quad (11)$$

Referring to Fig. 6, the upper and lower load capacity ratios (in per unit value p.u.) are denoted as  $r_A$  and  $r_B$ , respectively, with active and reactive power changing ratio of  $h_{sA}, h_{ca}$  and  $h_{sB}, h_{cb}$ , respectively. By substituting these boundary conditions into (11), the expressions in (12) can be obtained

$$\begin{cases} m_{LCa} = \frac{(h_{sA})(\sin \theta_{ca, rated}) - \sqrt{(h_{sA})^2(\sin \theta_{ca, rated})^2 + (k_{invaLC})^2 - 1}}{r_A} \\ m_{LCa} = \frac{(h_{sB})(\sin \theta_{ca, rated}) + \sqrt{(h_{sB})^2(\sin \theta_{ca, rated})^2 + (k_{invaLC})^2 - 1}}{r_B} \end{cases} \quad (12)$$

By further manipulation of (11), the middle point of the compensation range  $r_M$  can be determined according to (13) shown at the bottom of the page.

Since the railway HPQC coupled impedance cannot be changed easily once installed, the value of  $m_{LCa}$  is the same in (12). With the boundary loading conditions known, the two unknowns in (12) are mainly coupled impedance  $X_{LCa}$  and the operation voltage rating  $k_{invaLC}$ . Solving the expression for these two parameters yields the result in (14), which is the core equations for impedance-mapping railway HPQC. Notice that subscript “\_map” is added to signify that the parameters are determined by proposed impedance-mapping technique equation (5) and (14) shown at the bottom of the page.

As shown in [24], the value of  $m_{LCa}$  for minimum operation voltage design under fixed rated load is  $\sin \theta_{ca, rated}$ . Therefore, the expression of  $m_{LCa, map}$  in (14) may be revised as shown in (15). A modification factor  $g$  is used to define the modification of coupled impedance from rated one using proposed impedance-mapping technique

$$m_{LCa, map} = \left( \frac{2(r_A h_{sA} - r_B h_{sB})}{(r_A)^2 - (r_B)^2} \right) (\sin \theta_{ca, rated}) = g \cdot m_{LCa, min op} \quad (15)$$

When the value of the coupled impedance  $m_{LCa}$  is determined, the  $V_{ac}$  phase-coupled inductance may then be computed based on [25], which final determination expressions are shown in (16) and (17)

$$L_a = \frac{X_{La}}{\omega} = \frac{1}{\omega} \cdot k_L \cdot |X_{LCa}| = \frac{1}{\omega} \cdot k_L \cdot g \cdot m_{LCa, min op} \cdot \frac{V_{ac}}{I_{ca, rated}} \quad (16)$$

$$C_a = \frac{1}{\omega \cdot X_{ca}} = \frac{1}{\omega \cdot k_C \cdot |X_{LCa}|} = \frac{1}{\omega \cdot k_C \cdot g \cdot m_{LCa, min op}} \cdot \frac{I_{ca, rated}}{V_{ac}} \quad (17)$$

$$r_M = \frac{r_A + r_B}{2} = \frac{(h_{sA} + h_{sB}) \sin \theta_{ca, rated} - \sqrt{(h_{sA})^2(\sin \theta_{ca, rated})^2 + (k_{invaLC})^2 - 1} + \sqrt{(h_{sB})^2(\sin \theta_{ca, rated})^2 + (k_{invaLC})^2 - 1}}{2m_{LCa}} \quad (13)$$

$$\begin{cases} m_{LCa, map} = \frac{2(r_A h_{sA} - r_B h_{sB})(\sin \theta_{ca, rated})}{(r_A)^2 - (r_B)^2} \\ k_{invaLC, map} = \sqrt{(r_A \cdot m_{LCa, map})^2 - 2(r_A \cdot m_{LCa, map})(h_{sA} \cdot \sin \theta_{ca, rated}) + 1} \\ \quad = \sqrt{(r_B \cdot m_{LCa, map})^2 - 2(r_B \cdot m_{LCa, map})(h_{sB} \cdot \sin \theta_{ca, rated}) + 1} \end{cases} \quad (14)$$

where

$$k_L = \frac{\sum_{h=2}^{\infty} (r_h)^2 \cdot \frac{2(h^2 - 1)}{h^2}}{\sum_{h=2}^{\infty} (r_h)^2 \cdot \frac{2(h^2 - 1)^2}{h^2}}$$

and  $k_C = -1 - k_L$  according to the loading conditions.

Further deducing from (15), the value of impedance modification factor  $g$  can be determined by (18). This factor is useful for the following analysis:

$$g = \frac{2(r_A h_{sA} - r_B h_{sB})}{(r_A)^2 - (r_B)^2} \quad (18)$$

By substituting (18) into (12), the expression in (19), shown at the bottom of the page, can be obtained. The value of  $r_A$  and  $r_B$  can be changed by the factor  $g$ . The proposed impedance-mapping design technique therefore gives one more degree to freedom so that the railway HPQC can be designed based on required compensation range/capability. This is not achievable when  $g = 1$ .

### B. Analysis of Effectiveness in Operation Voltage Reduction

1) *Reduction in Operation Voltage Rating:* As discussed, proposed impedance-mapping technique is useful for reduction in railway HPQC operation voltage. This may be investigated by the ratio of operation voltage rating of impedance-mapping railway HPQC to that of railway HPQC developed based on minimum operation voltage at rated load. Referring to (14) and  $g = 1$  for minimum operation voltage design at rated load, the ratio can be determined as (20) shown at the bottom of the page.

Assuming that the load PF is constant during load variations such that  $h_s = 1$ , a MATLAB plot is constructed according to (20) and is shown in Fig. 8. Since the compensation range of railway HPQC for minimum operation voltage at rated load is always centered at 1.0, it can be observed that for load capacity ( $r$  or  $r_A$ ) lower than 0.65, the value of  $R_k$  is lower than 1.0, indicating that the operation voltage is reduced. The value of  $g$  and  $k_{invaLC}$  may then be selected according to desired compensation capability. For example, in the case that we investigate, the traction load capacity ranges from 0.2 to 1.2, the value of  $r_A$  is therefore located at 0.2, with  $R_k$  value of 0.96

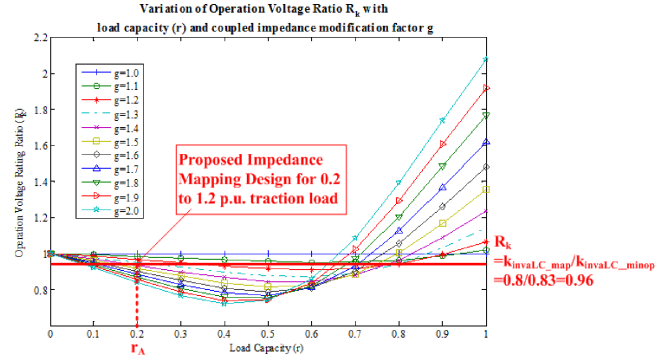


Fig. 8. MATLAB plot showing the relationship variation of operation voltage ratio  $R_k$  with load capacity ( $r$ ) and coupled impedance modification factor ( $g$ ) to show the effectiveness of reduction in operation voltage using proposed impedance-mapping railway HPQC.

using proposed impedance mapping design technique, as shown in the figure. This shows reduction of operation voltage using proposed technique.

2) *Criteria for Operation Voltage Rating Reduction:* It can be observed from Fig. 8 that the operation voltage rating of impedance-mapping railway HPQC may sometimes be larger than that derived for minimum operation voltage at rated load. The limitation criteria may be determined by further investigating the expression in (20). Reduction of operation voltage can be achieved when  $R_k < 1$ , the expression in (21) can then be obtained. Reduction in operation voltage is achievable using proposed impedance-mapping technique when (21) is satisfied. Otherwise, it is suggested to use conventional design parameter where  $g = 1$

$$r < \frac{2(g \cdot h_s - 1)}{g^2 - 1}. \quad (21)$$

### C. Analysis on Coupled Capacitance Reduction

1) *Reduction in Coupled Capacitance:* The reduction in coupled capacitance using proposed technique is analyzed later. Since the coupled impedance is inversely proportional to the equivalent coupled capacitance, as shown in (22), a larger value of  $X_{LCa}$  (and also  $m_{LCa}$ ) is therefore preferred for a lower

$$\begin{cases} r_A = \frac{(h_{sA}) (\sin \theta_{ca\_rated}) - \sqrt{(h_{sA})^2 (\sin \theta_{ca\_rated})^2 + (k_{invaLC})^2 - 1}}{g \cdot m_{LCa\_rated}} \\ r_B = \frac{(h_{sB}) (\sin \theta_{ca\_rated}) + \sqrt{(h_{sB})^2 (\sin \theta_{ca\_rated})^2 + (k_{invaLC})^2 - 1}}{g \cdot m_{LCa\_rated}} \end{cases} \quad (19)$$

$$\begin{aligned} R_k &= \frac{k_{invaLC\_map}}{k_{invaLC\_minop}} \\ &= \sqrt{\frac{(r \cdot g \cdot \sin \theta_{ca\_rated})^2 - 2(r \cdot g \cdot \sin \theta_{ca\_rated})(h_s \cdot \sin \theta_{ca\_rated}) + 1}{(r \cdot \sin \theta_{ca\_rated})^2 - 2(r \cdot \sin \theta_{ca\_rated})(h_s \cdot \sin \theta_{ca\_rated}) + 1}} \end{aligned} \quad (20)$$

coupled capacitance

$$C_{eq} = \frac{1}{\omega \cdot X_{LCa}} = \frac{I_{ca, rated}}{\omega \cdot m_{LCa} \cdot V_{ac}}. \quad (22)$$

It can be deduced from (6) and (15) that the coupled impedance of impedance mapping railway HPQC is  $g$  times that of railway HPQC derived based on minimum operation voltage. The ratio of equivalent coupled impedance is therefore  $1/g$ . These relationships are shown in (23) and (24)

$$X_{LCa, map} = g \cdot X_{LCa, min op} \quad (23)$$

$$C_{eq, map} = \frac{1}{g} \cdot C_{eq, min op}. \quad (24)$$

2) *Criteria for Coupled Capacitance Reduction*: The impedance-mapping railway HPQC coupled impedance can only be reduced when  $1/g < 1$ . Combining with (18), it can be concluded that the expression in (25) must be satisfied so that reduction in coupled capacitance can be achieved using impedance-mapping method

$$\frac{2(r_A h_{sA} - r_B h_{sB})}{(r_A)^2 - (r_B)^2} > 1 \quad (25)$$

#### D. Example Studies

In order to explain the analysis, two loading conditions are being investigated later. They are developed mainly based on the practical WuQing substation data in China.

1)  $r_A = 0.2$ ,  $r_B = 1.2$ ,  $h_{sA} = h_{sB} = 1$  (*WuQing Substation Data, Constant Load PF*): According to the WuQing substation data, the load capacity ranges from 0.2 to 1.1 p.u. Assuming the load PF is kept constant,  $h_{sA} = h_{sB} = 1.0$ . By substituting  $r_A = 0.2$ ,  $r_B = 1.2$ ,  $h_{sA} = h_{sB} = 1$  into (18), it can be computed that the value of  $g$  is around 1.43. By substituting  $g = 1.43$  into (21), it is found that reduction in operation voltage can be achieved since the value of  $r$  (or  $r_A$ ) is lower than 0.82. According to (20), there is around 9% reduction in operation voltage.

With  $g = 1.43$ , the expression in (25) is satisfied, and by substituting the values into (24), it is found that there is nearly 30% reduction in coupled capacitance.

2)  $r_A = 0.2$ ,  $r_B = 1.2$ ,  $h_{sA} = 1.03$ ,  $h_{sB} = 0.96$  (*WuQing Substation Data,  $PF_L = 0.8-0.9$* ): Still referring to WuQing substation traction data, the load capacity is 0.2 to 1.2 p.u., but it is further assumed that the load PF ranges from 0.8 (condition A) to 0.9 (condition B) such that  $h_{sA} = 1.03$ ,  $h_{sB} = 0.96$ . By substituting  $r_A = 0.2$ ,  $r_B = 1.2$ ,  $h_{sA} = 1.03$ ,  $h_{sB} = 0.96$  into (18), it can be computed that the value of  $g$  is 1.52. Substituting  $g = 1.52$  into (21), it can also be found that the condition is satisfied and a nearly 10% reduction in operation voltage can be achieved using impedance-mapping railway HPQC according to (20).

With  $g = 1.52$ , the expression in (25) is also satisfied, and by substituting the values into (24), it is found that there is nearly 34% reduction in coupled capacitance.

A summary of the analysis carried out earlier is shown in Table I to show the reduction in operation voltage rating and

TABLE I  
SUMMARY OF THE REDUCTION IN OPERATION VOLTAGE RATING  $k_{invaLC}$  AND COUPLED CAPACITANCE  $C_{eq}$  USING PROPOSED IMPEDANCE-MAPPING RAILWAY HPQC DESIGN (TWO CASES)

	$r_A$	$r_B$	$h_{sA}$	$h_{sB}$	$g$	$\Delta k_{invaLC}$	$\Delta C_{eq}$
Case A	0.2	1.2	1	1	1.43	-9%	-30%
Case B	0.2	1.2	1.03	0.96	1.52	-10%	-34%

coupled impedance using proposed impedance-mapping railway HPQC design in this paper.

These two example condition shows that reduction in operation voltage and coupled capacitance can be achieved by proposed impedance-mapping railway HPQC.

#### V. PROPOSED IMPEDANCE MAPPING RAILWAY HPQC DESIGN PROCEDURES

Referring to the earlier analysis, the proposed impedance mapping HPQC design is then shown later. Notice that in contrast to railway HPQC designed for minimum operation voltage at rated load, as soon as the conditions in (21) and (25) are satisfied, the coupled impedance of railway HPQC can be designed based on required compensation range/capability using proposed impedance-mapping technique for reduction in operation voltage and coupled capacitance. Here are details of proposed design:

- 1) record the boundary conditions of normal load capacity rating (p.u.) and denote the lower one as  $r_A$ , and larger one as  $r_B$ ;
- 2) record also the load PF and compute the value of  $h_s$  at boundary conditions according to (2) and (3); denote the lower boundary one as  $h_{sA}$  and the upper boundary one as  $h_{sB}$ ;
- 3) map the  $V_{ac}$  coupled impedance  $X_{LCa}$  in railway HPQC with the desired loading variation range (compensation range) according to (26)

$$\begin{aligned} |X_{LCa}| &= m_{LCa, map} \cdot \left( \frac{V_{ac}}{I_{ca, rated}} \right) \\ &= g \cdot m_{LCa, min op} \cdot \left( \frac{V_{ac}}{I_{ca, rated}} \right) \\ &= \frac{2(r_A h_{sA} - r_B h_{sB})}{(r_A)^2 - (r_B)^2} \cdot (\sin \theta_{ca, rated}) \cdot \left( \frac{V_{ac}}{I_{ca, rated}} \right) \end{aligned} \quad (26)$$

- 4) compute to determine the  $V_{ac}$  phase-coupled inductance and capacitance according to (16) and (17);
- 5) compute the required HPQC operation voltage according to (14);
- 6) determine the  $V_{bc}$  phase-coupled impedance according to (27)

$$\begin{aligned} X_{LCb} &= \frac{V_{bc} \sin \theta_{cb} + \sqrt{V_{invaLC}^2 - V_{bc}^2 \cos^2 \theta_{cb}}}{I_{cb}} \\ &= \frac{V_{bc} \sin \theta_{cb} - \sqrt{V_{invaLC}^2 - V_{bc}^2 \cos^2 \theta_{cb}}}{I_{cb}}. \end{aligned} \quad (27)$$

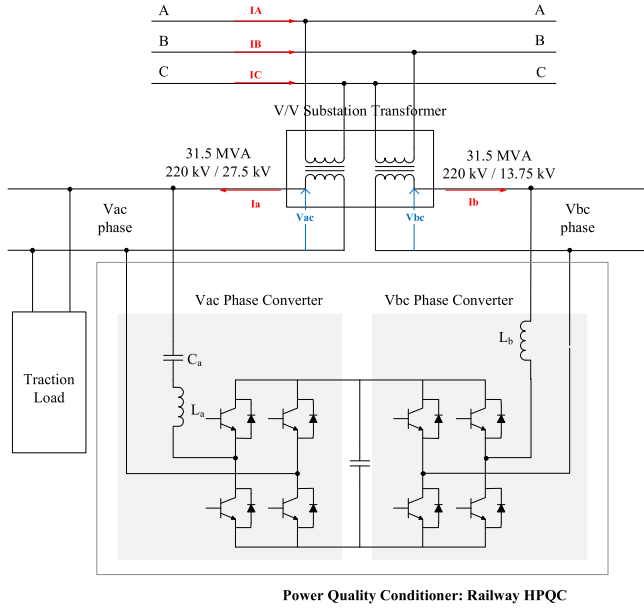


Fig. 9. Circuit schematic of the co-phase traction power in PSCAD simulation verifications.

## VI. SIMULATION VERIFICATIONS BASED ON PRACTICAL DATA OF WUQING SUBSTATION

Simulations verifications are done using PSCAD to show the reduction of operation voltage and coupled capacitance using proposed impedance-mapping railway HPQC for providing compensation in co-phase traction power within the designed load variation range. Shown in Fig. 9 is the simulation circuit schematic of the co-phase traction power supply under investigation. Practical loading conditions are taken into consideration to simulate real implementation. The circuit structure resembles that of China WuQing Substation (refer to the Appendix), except that the co-phase technique is adopted. The substation transformer is in V/V connection, and is composed of two single-phase transformers, each of 31.5 MVA. As described previously, in co-phase traction power, the traction load is connected across  $V_{ac}$  phase only and the power quality conditioner, railway HPQC, is connected across  $V_{ac}$  and  $V_{bc}$  phase to provide compensation. The voltage of  $V_{ac}$  is 27.5 kV and that of  $V_{bc}$  is 13.75 kV through step-down substation transformer. For verification of the theory and impedance-mapping design method, railway HPQC in a two-level structure is being studied. But the theory may be extended to be applied in a multilevel structure.

The simulation is performed with various loading capacities. With rated capacity at 31.5 MVA, the traction load capacity ranges from 6.5 to 36.5 MVA (0.2–1.2 p.u.), which is 0.21 to 1.16 in per unit value. Details of the loading condition may be found in the Appendix. It is further assumed that similar to other traction loadings, the load PF is around 0.85. The traction load model in the simulation is mainly used to simulate the presence of reactive power and harmonics in traction load. In the verification, the traction load is simulated using rectifier RLC load, with load capacity range of 0–2.0 p.u. It is further

TABLE II  
RAILWAY HPQC DESIGN WITH MINIMUM OPERATION VOLTAGE FOR RATED LOAD OF WUQING SUBSTATION BASED ON MINIMUM OPERATION VOLTAGE REQUIREMENT

Parameters	Descriptions	Value
$I_{ca, rated}$	$V_{ac}$ phase compensation current	1000 A
PFL	Load PF	0.85
$\theta_{ca}$	$V_{ac}$ phase Compensation Angle	61.28
$g$	$V_{ac}$ phase-coupled impedance ratio modification factor	1.0
$m_{LCa}$	$V_{ac}$ coupled impedance ratio	0.87
$L_a$	$V_{ac}$ coupled inductance	7.46 mH
$C_a$	$V_{ac}$ coupled capacitance	123 $\mu$ F
$k_{invaL}$	Railway HPQC operation voltage rating	0.83
$V_{dc}$	DC-link voltage	34.5 kV

assumed that the load capacity varies with constant load PF such that  $h_s = h_c = 1.0$ .

The performance of railway HPQC with the following two conditions is being investigated: 1) railway HPQC developed based on minimum operation voltage rating at rated load; and 2) railway HPQC using proposed impedance-mapping design for operation voltage and coupled capacitance reduction. The three-phase system source PF, current unbalance, and total harmonics distortions (THD) are monitored according to the IEEE standard. The main goal of railway HPQC under this simulation verification is to provide satisfactory compensation performance within the designed load variation range (0.2 to 1.2 p.u.) (THD < 10%, PF > 0.98).

### A. Railway HPQC Developed Based on Minimum Operation Voltage Rating at Rated Load ( $V_{dc} = 34.5$ kV)

Simulations are first done with HPQC using minimum operation voltage design based on rated load. The  $V_{ac}$  coupled impedance ratio  $m_{LCa}$  and railway HPQC operation voltage rating is designed according to [24]. Details of HPQC design and component parameters can be found in Table II.

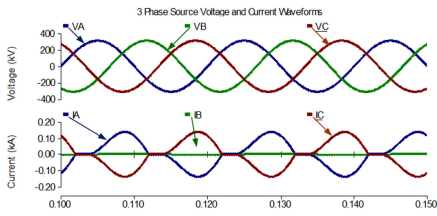
### B. Simulation With Railway HPQC Using Proposed Impedance Mapping Design Based on Required Compensation Capability ( $r_A = 0.2$ , $r_B = 1.2$ , $h_s = 1$ , $h_c = 1$ , $V_{dc} = 31.5$ kV)

Next, simulation results are obtained with railway HPQC using proposed impedance mapping design based on required compensation range/capability. In contrast with minimum operation voltage HPQC design, the HPQC is designed to provide satisfactory compensation for desired load capacity of 0.2 to 1.2 p.u. Assuming that the load capacity varies with fixed rated load PF, the  $V_{ac}$  coupled impedance ratio  $m_{LCa}$  and railway HPQC operation voltage rating may be designed according to (14) and the procedures in Section IV. The HPQC parameters with proposed design are presented in Table III. Notice that the operation voltage 31.5 kV is lower than the peak PCC traction load voltage (39 kV). This dc link operation voltage is also lower than that in traditional RPC (41 kV).

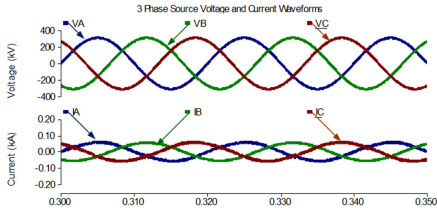
The simulated system waveforms are shown in Fig. 10. Four conditions are mainly presented, namely: 1) outside designed compensation range near no-load conditions (0.1 p.u.); 2) within

**Load Capacity: 1.0 p.u. (Rated Load)**

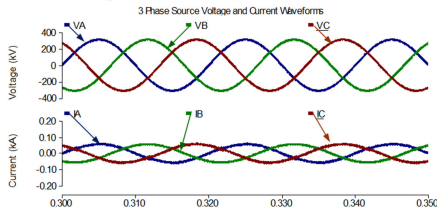
Before Compensation



With Railway HPQC Compensation based on Minimum Operation Voltage at Rated Load ( $V_{dc}=34.5$  kV)



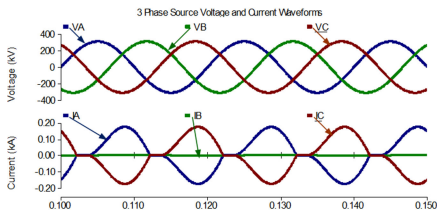
With proposed impedance-mapping Railway HPQC based on Load Range ( $V_{dc}=31.5$  kV)



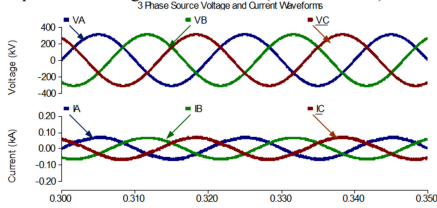
(c)

**Load Capacity: 1.3 p.u. (outside range)**

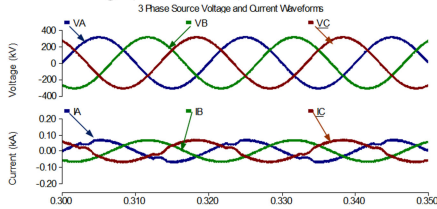
Before Compensation



With Railway HPQC Compensation based on Minimum Operation Voltage at Rated Load ( $V_{dc}=34.5$  kV)



With proposed impedance-mapping Railway HPQC based on Load Range ( $V_{dc}=31.5$  kV)



(d)

Fig. 10. Simulated co-phase traction power system waveforms under different load rating and simulation conditions: (a) 0.1 p.u.; (b) 0.6 p.u.; (c) 1.0 p.u.; and (d) 1.3 p.u.

TABLE III

DETAILED PARAMETERS OF PROPOSED IMPEDANCE MAPPING RAILWAY HPQC DESIGN FOR 0.2–1.2 P.U. TRACTION LOAD CAPACITY VARIATION RANGE

Parameters	Descriptions	Value
$r_a$	Load capacity ratio	0.2
$r_b$	Load capacity ratio	1.2
$I_{ca}$	$V_{ac}$ phase compensation current	1000 A
PFL	Load PF	0.85
$\theta_{ca}$	$V_{ac}$ phase compensation angle	61.28
$g$	$V_{ac}$ phase-coupled impedance ratio modification factor	1.44
$m_{Lca}$	$V_{ac}$ coupled impedance ratio	1.26
$L_a$	$V_{ac}$ coupled inductance	10.9 mH
$C_a$	$V_{ac}$ coupled capacitance	84 $\mu$ F
$k_{inv aL}$	Railway HPQC operation voltage rating	0.79
$V_{dc}$	DC-link voltage	31.5 kV

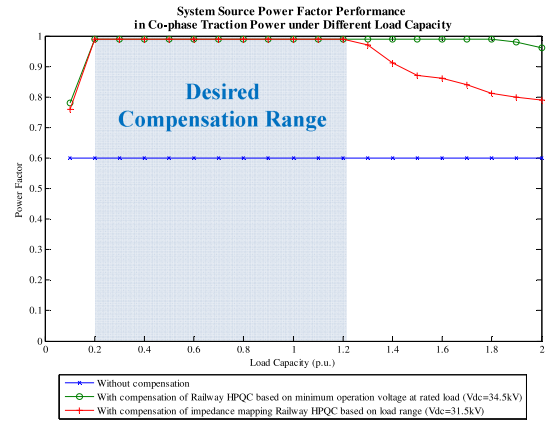


Fig. 11. Simulated system source PF performance in co-phase traction power under different load capacity.

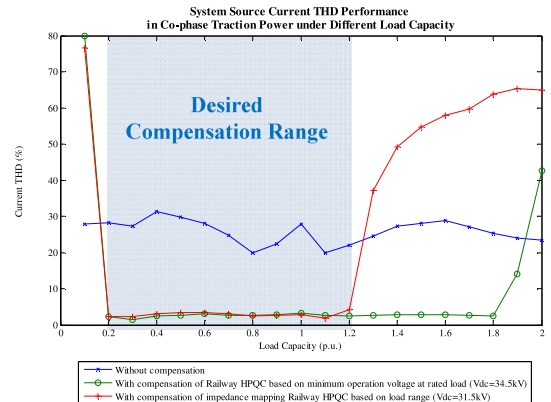


Fig. 12. Simulated system source current THD performance in co-phase traction power under different load capacity.

designed compensation range (0.6 p.u.); 3) within designed compensation range at rated load (1.0 p.u.); and 4) outside designed compensation range at over load (1.3 p.u.). More simulation performance of source PF, current harmonic distortions, and system unbalance under different load capacity are shown in Figs. 11–13.

It can be observed from the figure that for railway HPQC developed based on minimum operation at rated load, the compensation performance is satisfactory even when outside the

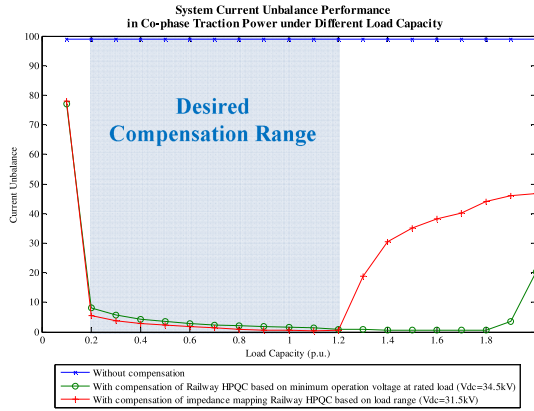


Fig. 13. Simulated system source current unbalance performance in co-phase traction power under different load capacity.

compensation range (0.1, 1.3 p.u.), indicating that the compensation capability is more than enough. This causes high excessive operation voltage and coupled capacitance. On the other hand, with proposed impedance-mapping technique in railway HPQC, satisfactory compensation performance within the load range (0.2 to 1.2 p.u.), but with a 9% reduction in operation voltage. Moreover, there is around 30% reduction in the coupled capacitance. This is consistent with previous analysis and shows the effectiveness of proposed impedance-mapping railway HPQC in reducing operation voltage and coupled capacitance. Notice that the system performance is more or less the same within the load variation range (0.2 to 1.2 p.u.).

### C. Performance of Railway HPQC Using Proposed Impedance-Mapping Technique Under Step Load Change

Next, the performance of railway HPQC using proposed impedance-mapping design under step load condition change is investigated. It is assumed that the load capacity is changed from 0.6 p.u. (middle of compensation range) to 1.0 p.u. (rated load) at 0.4 second. The simulated system waveforms are shown in Fig. 14. It can be observed the power quality compensation performance is both satisfactory.

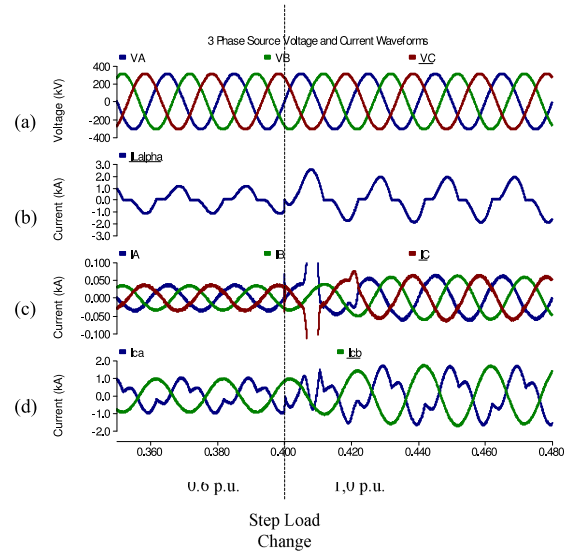


Fig. 14. Simulated system waveforms of co-phase traction power supply with railway HPQC using proposed impedance-mapping design technique: (a) system source voltage; (b) traction load current; (c) system source current; and (d)  $V_{ac}$  phase and  $V_{bc}$  phase compensation current.

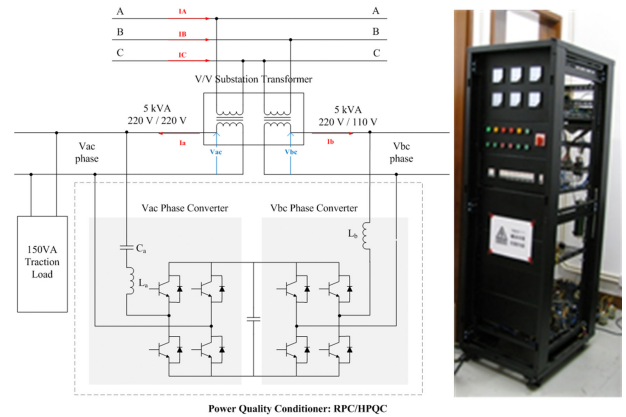


Fig. 15. Circuit schematics and appearance of the laboratory scaled hardware prototype of 150VA co-phase traction power supply system.

## VII. EXPERIMENTAL RESULTS

In order to further verify the proposed impedance-mapping design of railway HPQC based on load range, experimental results are obtained from a laboratory scaled co-phase traction power supply system. For safety concern in laboratories, the traction load voltage used is scaled down by 1:550 compared to practical 27.5 kV system. Detailed circuit schematics and hardware appearance is shown in Fig. 15. It is also assumed that the desired load/compensation range is 0.2 to 1.2 p.u., which is the same as the one at WuQing substation. The three-phase source power quality is being monitored and the results obtained using HPQC with proposed impedance mapping design are presented later to show its validity.

The HPQC is designed according to the proposed impedance mapping method within this document. Detailed HPQC parameter design used in the experiment is presented in Table IV.

TABLE IV  
PROPOSED HPQC PARAMETER DESIGN USED IN EXPERIMENT FOR 0.2–1.2 P.U. TRACTION LOAD CAPACITY

Parameters	Descriptions	Value
$r_A$	Load capacity ratio	0.2
$r_B$	Load capacity ratio	1.2
$I_{ca}$	$V_{ac}$ phase compensation current	2.65 A
PFL	Load PF	0.85
$\theta_{ca}$	$V_{ac}$ phase compensation angle	61.28
$g$	$V_{ac}$ phase-coupled impedance ratio modification factor	1.44
$m_{L,a}$	$V_{ac}$ coupled impedance ratio	1.25
$L_a$	$V_{ac}$ coupled inductance	7.9 mH
$C_a$	$V_{ac}$ coupled capacitance	122 $\mu$ F
$k_{invaL}$	Railway HPQC operation voltage rating	0.79
$V_{dc}$	DC-link voltage	57 V

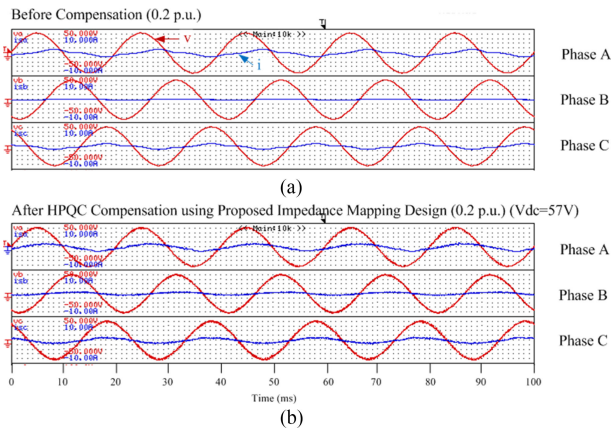


Fig. 16. Hardware experimental source voltage and current waveforms obtained under 0.2 p.u. loading condition.

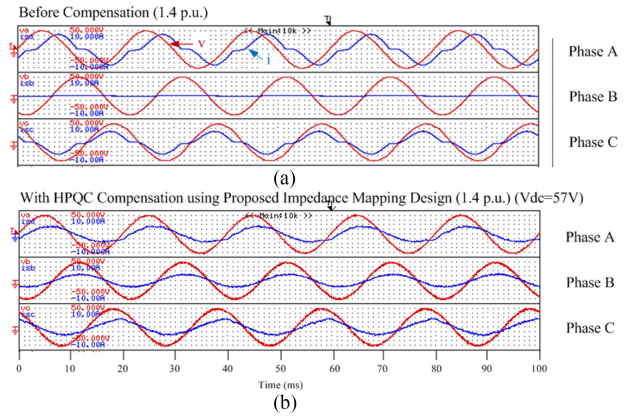


Fig. 19. Hardware experimental source voltage and current waveforms obtained under 1.4 p.u. loading condition.

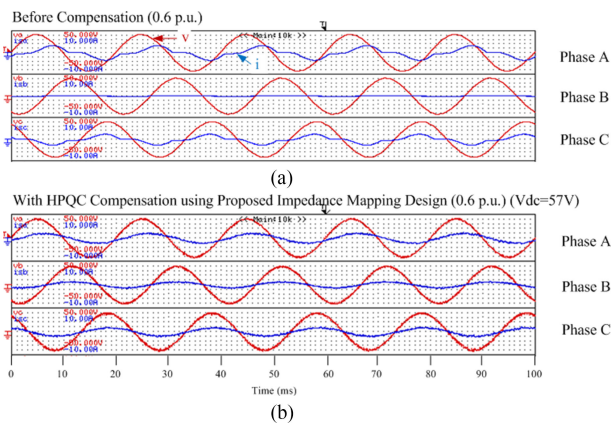


Fig. 17. Hardware experimental source voltage and current waveforms obtained under 0.6 p.u. loading condition.

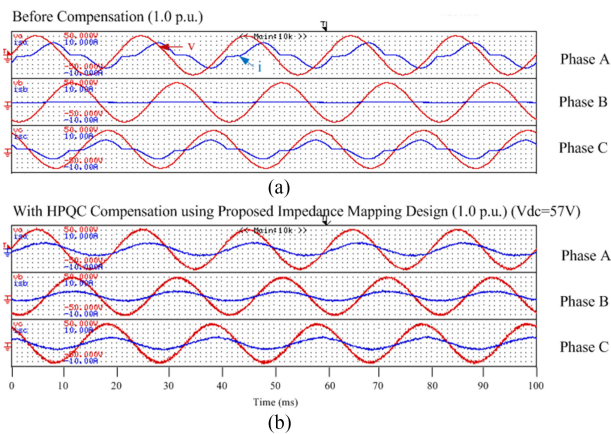


Fig. 18. Hardware experimental source voltage and current waveforms obtained under 1.0 p.u. loading condition.

Hardware results are obtained under 0.2 to 1.4 p.u. load for each 0.2 p.u. Some captured waveforms are shown in Figs. 16–19 for loading condition of 0.2, 0.6, 1.0, and 1.4 p.u. The reasons for showing these waveforms are to show typical conditions within and outside the designed load range. It can be seen from the figures that within the designed load range (0.2–1.2 p.u.), the performance is satisfactory, and outside the

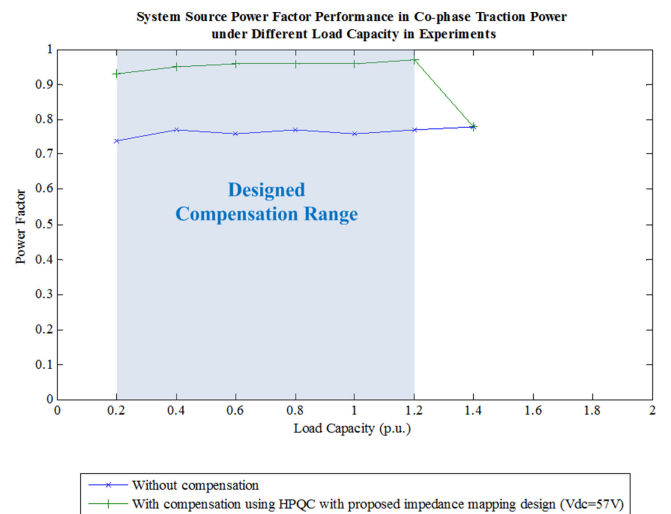


Fig. 20. Experimental performance of system source PF in co-phase traction power under different load capacity (a) without compensation; (b) with compensation using HPQC with proposed design ( $V_{dc} = 57$  V).

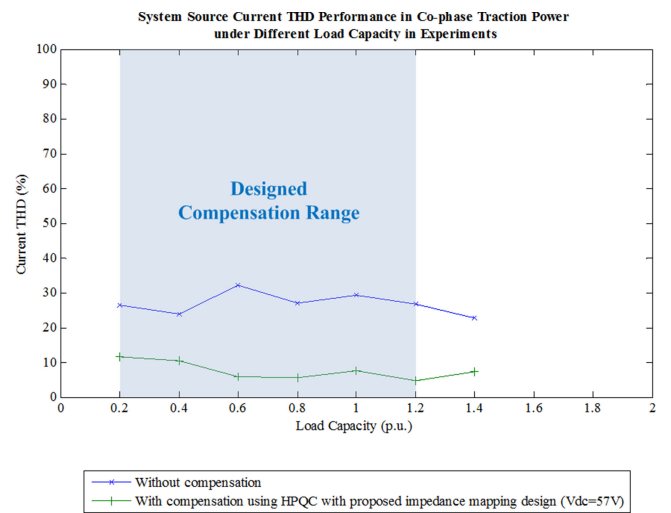


Fig. 21. Experimental performance of system source current THD in co-phase traction power under different load capacity (a) without compensation; (b) with compensation using HPQC with proposed impedance mapping design ( $V_{dc} = 57$  V).

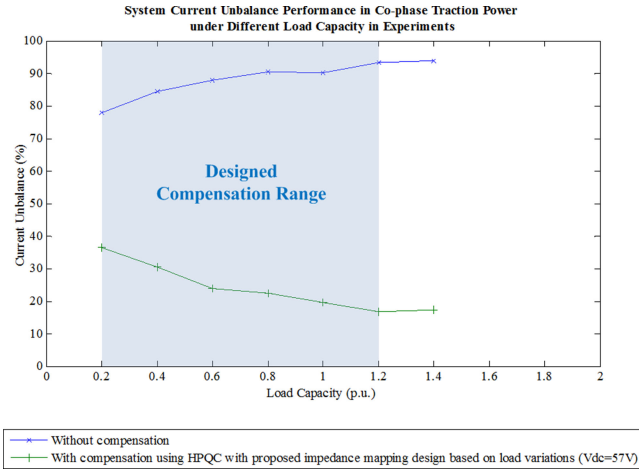


Fig. 22. Experimental performance of system source current unbalance in co-phase traction power under different load capacity (a) without compensation; (b) with compensation using HPQC with proposed impedance mapping design ( $V_{dc} = 57$  V).

compensation range, distortions are found in the waveforms. Detailed compensation performances of system source current unbalance, harmonic distortions and PF under the loading condition investigated are presented in Figs. 20–22. It can be clearly shown that the compensation performance is satisfactory within the designed compensation range using railway HPQC with the proposed design. This then shows the validity of the proposed impedance-mapping design technique to provide satisfactory compensation performance for desired compensation range/capability. Moreover, the railway HPQC operation voltage using proposed impedance mapping design is still lower the conventional RPC operation voltage.

### VIII. CONCLUSION

In this paper, the effect of co-phase railway HPQC coupled impedance on compensation capability is being analyzed and a novel impedance-mapping design technique according to required capability is proposed based on the analysis. The proposed impedance-mapping design technique is beneficial for reduction in operation voltage and coupled capacitance while providing satisfactory compensation performance for a desired range of loadings in co-phase high-speed power supply. Details of the theoretical derivations and analysis on the operation voltage and coupled capacitance using impedance-mapping railway HPQC are covered in this paper. Practical WuQing substation data are used to perform PSCAD simulation verifications. It is found that there is 9% reduction in operation voltage and 30% reduction in coupled capacitance compared to railway HPQC design in previous works. The system performance is satisfactory and is more or less the same within load variation range. A lab-scaled hardware prototype is also constructed and the performance of newly proposed impedance-mapping railway HPQC is verified. Reduction of operation voltage and coupled capacitance reduces the cost. Moreover, the proposed impedance-mapping design technique may also be extended to other applications of hybrid  $LC$  coupled converter in which active

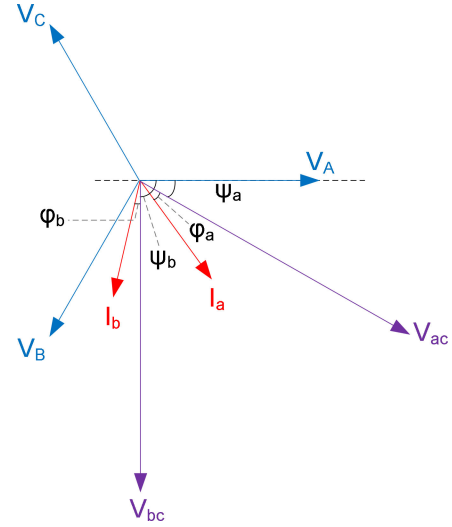


Fig. A1. Vector definition in the derivation of required power.

and reactive power transfer is involved, such as the renewable energy converters in smart grid.

### APPENDIX

In order to maintain the focus of the paper, the following parts are shown as appendix, including the derivation of the RPC/railway HPQC control algorithm as well as details of the practical WuQing substation data.

#### A. Derivation of the Control Algorithm in Co-phase Traction Power Quality Conditioner

No matter which power quality conditioner, either conventional RPC or newly proposed railway HPQC, is being used, power quality compensation is provided to the primary source from transformer secondary side (load side). Since the ultimate goal of the power quality conditioner is to provide power quality compensation at the grid side, it is very important that the power quality parameter at grid side is being modeled using the parameters at the transformer secondary side. The required output compensation power and thus current from the power quality conditioner can then be determined based on the power quality requirement. Details of the derivation may be referred in (reference). Some key equations and ideas are presented in this appendix to give readers a clear picture.

First, it is essential to define the parameters within the analysis. The derivation is performed based on the parameter definition in Fig. 2. Shown in Fig. A1 is a vector diagram showing the definition of the parameters in the derivation.

The  $V_{ac}$  and  $V_{bc}$  phase voltage and current are defined as shown in (A1)

$$\begin{cases} \dot{V}_{ac} = V_{ac} e^{-j\psi_a} & \dot{I}_a = I_a e^{-j(\psi_a + \phi_a)} \\ \dot{V}_{bc} = V_{bc} e^{-j\psi_b} & \dot{I}_b = I_b e^{-j(\psi_b + \phi_b)} \\ |V_{bc}| = |V_{ac}| \end{cases} \quad (A1)$$

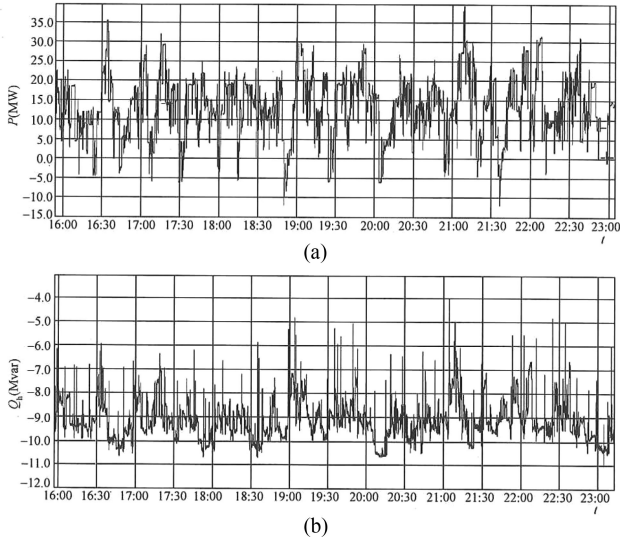


Fig. A2. Graph showing the active and reactive power obtained from the 24-hour continuous monitoring at WuQing substation.

For the system unbalance, it is being modeled using method of symmetrical components. It is stated in IEEE standard that the presence of negative sequence indicates system unbalance and system unbalance may be represented as a ratio of negative sequence to fundamental components. The derived model of negative sequence current  $I^-$  and positive- and zero-sequence current  $I^+$  and  $I^0$  are shown in (A2)

$$\begin{cases} \dot{I}^0 = 0 \\ \dot{I}^- = \frac{1}{\sqrt{3}K} [I_a e^{-j(\psi_a + \phi_a)} \cdot e^{-j30^\circ} + I_b e^{-j(\psi_b + \phi_b)} \cdot e^{-j90^\circ}] \\ \dot{I}^+ = \frac{1}{\sqrt{3}K} [I_a e^{-j(\psi_a + \phi_a)} \cdot e^{+j30^\circ} + I_b e^{-j(\psi_b + \phi_b)} \cdot e^{+j90^\circ}] \end{cases} \quad (\text{A2})$$

The PF of the three-phase source grid, PFA, PFB, and PFC for phases A, B, and C, respectively, can be derived mathematically, as shown in (A3)

$$\text{PFA} = \cos(0^\circ + \psi_a + \phi_a)$$

$$\text{PFB} = \cos(-120^\circ + \psi_b + \phi_b)$$

$$\text{PFC} = \cos\left(-240^\circ + \tan^{-1}\left(\frac{I_a \sin \varphi_a + I_b \sin \varphi_b}{-I_a \cos \varphi_a - I_b \cos \varphi_b}\right)\right). \quad (\text{A3})$$

As for the harmonics, they can be compensated by compensating with the ac portion of instantaneous active power and all instantaneous reactive power.

The power quality at the three-phase source grid side in phase traction power with V/V transformer can then be modeled using (A4). However, the equations in (A4) are still not enough to derive the required output compensation power of the power quality conditioner since there are too many unknowns equation (A4) is shown bottom of the page.

$$\text{where } \varphi_a = \psi_a + \phi_a \text{ and } \varphi_b = \psi_b + \phi_b$$

Therefore, another equation, shown in (A5), is added during the derivation. It reflects the fact that no active power is being stored in the power quality conditioner during compensation

$$I_a \cos \phi_a + I_b \cos \phi_b = I_L \cos \phi_L = I_{Lp}. \quad (\text{A5})$$

The required power quality compensation power can then be computed by further manipulations according to the power quality requirements. For instance, for ideal compensation of  $\text{PFA} = \text{PFB} = \text{PFC} = 1$ ,  $I^- = 0$ ,  $I_h = 0$ , the required active and reactive power output  $p$  and  $q$ , of  $V_{ac}$  and  $V_{bac}$  phase (symbolized by ac and bc respectively), are shown in (A6)

$$\begin{bmatrix} p_{ca} \\ q_{ca} \\ p_{cb} \\ q_{cb} \end{bmatrix} = \begin{bmatrix} 0.5\bar{p}_L + \tilde{p}_L \\ 0.2887\bar{p}_L + q_L \\ -0.5\bar{p}_L \\ -0.2887\bar{p}_L \end{bmatrix}. \quad (\text{A6})$$

For example, the compensation control algorithm within this paper is developed based on (A6).

### B. Details of WuQing Practical Traction Data

It is already stated that the simulations within this paper are performed based on the data obtained from the WuQing substation in China. In 2009, an analysis is done by the China Electric Power Research Institute to investigate the Beijing-Tianjin high-speed railway. The data are obtained by monitoring the power quality of the substation for 24 hours continuously. Details can be found in the Appendix section.

First, the circuit structure of WuQing substation power supply is introduced. Similar to most existing traction power supplies, the 220 kV three-phase power is transformed into two single-phase 27.5 kV outputs through substation transformer. The WuQing substation transformer is composed of two single-phase transformers, with V/V connection. Each transformer is

$$\begin{cases} \text{PFA} = \cos(30^\circ + \phi_a) \\ \text{PFB} = \cos(-30^\circ + \phi_b) \\ \text{PFC} = \cos\left(-240^\circ + \tan^{-1}\left(\frac{I_a \sin \varphi_a + I_b \sin \varphi_b}{-I_a \cos \varphi_a - I_b \cos \varphi_b}\right)\right) \\ \text{Unbalance: } |I^-| = \frac{1}{\sqrt{3}K} \sqrt{I_a^2 + I_b^2 + 2I_a I_b \cos(-120^\circ + \phi_a - \phi_b)} \\ I_h = \sqrt{\sum_{n=2}^{\infty} I_n^2} \end{cases} \quad (\text{A4})$$

TABLE A1  
DATA EXTRACTED FROM FIG. A2 FOR FURTHER ANALYSIS AND INVESTIGATION  
WITHIN THIS REPORT

	Minimum	Maximum	Rated
Active Power $ P $ (MW)	0.0	35.0	=
Reactive Power $ Q $ (MVar)	6.0	10.5	=
Total Capacity (MVA)	6.0	36.5	31.5
Total Capacity (p.u.)	0.2	1.15	1.0

of 31.5 MVA capacity, and the locomotives are electrified with 27.5 ac power output of the transformer secondary side.

The active and reactive power data obtained from the 24-hour continuous monitoring at WuQing substation are shown in Fig. A2. Useful data are then extracted from the figure and can be found in Table A1. The minimum and maximum load capacity is used to determine the loading capacity range for the design of railway HPQC.

The data are then used for the design of railway HPQC in the paper. It is assumed that the traction load capacity ranges from 0.2 to 1.2 p.u. and details of railway HPQC design according to this assumption are presented in the main content.

#### ACKNOWLEDGMENT

The authors would like to thank Macao Science and Technology Development Fund (FDCT), the University of Macau Research Committee, and the University of Macau Electric Power Engineering Lab and colleagues, especially Tao Ye and JingJing Sheng, for their support in this research work.

#### REFERENCES

- [1] S. M. M. Gazafri, A. TabakhpourLangerudy, E. F. Fuchs, and K. Al-Haddad, "Power quality issues in railway electrification: A comprehensive perspective," *IEEE Trans Ind. Electron.*, vol. 62, no. 5, pp: 3081–3090, May. 2015.
- [2] P. Amrutha Paul, U. D. Anju, M. P. Anoop, M. RajanPallan, N. K. Roshna, and A. Sunny, "Effects of two phase traction loading on a three phase power transformer," in *Annu. Int. Conf. Emerg. Res. Areas: Magn., Mach. Drives*, 2014, pp. 1–5.
- [3] V. P. Joseph and J. Thomas, "Power quality improvement of AC railway traction using railway static power conditioner a comparative study," in *Proc. Int. Conf. Power Signals Contr. Comput.*, 2014, pp. 1–6.
- [4] P. E. Sutherland, M. Waclawiak, and M. F. Mcgranaghan, "System impacts evaluation of a single-phase traction load on a 115-kV transmission system," *IEEE Trans. Power Del.*, vol. 21, no. 2, pp: 837–844, Apr. 2006.
- [5] *IEEE Recommended Practice and Requirements for Harmonic Control in Electric Power Systems*, IEEE Std. 519-2014 (Revision of IEEE Std 519-1992), 2014.
- [6] P.-C. Tan, P. C. Loh, and D. G. Holmes, "Optimal impedance termination of 25-kV electrified railway systems for improved power quality," *IEEE Trans. Power Del.*, vol. 20, no. 2, pp: 1703–1710, Apr. 2005.
- [7] R. Grünbaum, J. Hasler, and B. Thorvaldsson, "FACTS: Powerful means for dynamic load balancing and voltage support of AC traction feeders" in *Proc. 2001 IEEE Porto Power Tech. Proc.*, vol. 4, p. 1.
- [8] H. F. Brown and R. L. Witzke, "Shunt capacitor installation for single phase railway service," *Trans. Amer. Inst. Electr. Eng.*, vol. 67, no. 1, pp. 258–266, 1948.
- [9] A. Bueno, J. M. Aller, J. A. Restrepo, R. Harley, and T. G. Habetler, "Harmonic and unbalance compensation based on direct power control for electric railway systems," *IEEE Trans. Power Electron.*, vol. 28, no. 12, pp. 5823–5831, Dec. 2013.
- [10] G. Celli, F. Pilo, and S. B. Tennakoon, "Voltage regulation on 25 kV AC railway systems by using thyristor switched capacitor" in *Proc. 9th Int. Conf. Harmonics Quality Power*, 2000, vol. 2, pp. 633–638.
- [11] C. Wu, A. Luo, J. Shen, F. J. Ma, and S. Peng, "A negative sequence compensation method based on a two-phase three-wire converter for a high-speed railway traction power supply system," *IEEE Trans. Power Electron.*, vol. 27, no. 2, pp: 706–717, Feb. 2012.
- [12] Z. Shu, S. Xie, and Q. Li, "Single-phase back-to-back converter for active power balancing, reactive power compensation, and harmonic filtering in traction power system," *IEEE Trans. Power Electron.*, vol. 26, no. 2, pp. 334–343, Feb. 2011.
- [13] Z. Sun, X. Jiang, D. Zhu, and G. Zhang, "A novel active power quality compensator topology for electrified railway," *IEEE Trans. Power Electron.*, vol. 19, no. 4, pp. 1036–1042, Jul. 2004.
- [14] L. Battistelli, M. Pagano, and D. Proto, "2 x 25-kV 50 Hz high-speed traction power system: Short-circuit modeling," *IEEE Trans. Power Del.*, vol. 26, no. 3, pp. 1459–1466, Jul. 2011.
- [15] L. Battistelli, D. Lauria, and D. Proto, "Two-phase controlled compensator for alternating-current quality improvement of electrified railway systems," *IEE Proc. Elect. Power Appl.*, vol. 153, no. 2, pp. 177–183, 2006.
- [16] M. Chen, Q. Z. Li, and G. Wei, "Optimized design and performance evaluation of new cophase traction power supply system" in *Proc. Asia-Pacific Power Energy Eng. Conf.*, 2009, pp. 1–6.
- [17] Z. Shu, S. Xie, and Q. Li, "Single-phase back-to-back converter for active power balancing, reactive power compensation, and harmonic filtering in traction power system," *IEEE Trans. Power Electron.*, vol. 26, no. 2, pp. 334–343, Feb. 2011.
- [18] Z. Shu, S. Xie, and Q. Z. Li, "Development and implementation of a prototype for co-phase traction power supply system," in *Proc. Asia-Pacific Power Energy Eng. Conf.*, 2010, pp. 1–4.
- [19] Q. Li, W. Liu, Z. Shu, S. Xie, and F. Zhou, "Co-phase power supply system for HSR," in *Proc. 2014 Int. Power Electron. Conf., IPEC-Hiroshima 2014 ECCE-ASIA*, pp. 1050–1053.
- [20] Z. Shu, S. Xie, K. Lu, Y. Zhao, X. Nan, D. Qiu, F. Zhou, S. Gao, and Q. Li, "Digital detection, control, and distribution system for co-phase traction power supply application," *IEEE Trans. Ind. Electron.*, vol. 60, no. 5, pp. 1831–1839, 2013.
- [21] N. Y. Dai, K. W. Lao, M. C. Wong, and C. K. Wong, "Hybrid power quality conditioner for co-phase power supply system in electrified railway," *Power Electron. IET*, vol. 5, no. 7, pp. 1084–1094, Aug. 2012.
- [22] N.-Y. Dai, M.-C. Wong, K.-W. Lao, and C.-K. Wong, "Modelling and control of a railway power conditioner in co-phase traction power system under partial compensation," *Power Electron. IET*, vol. 7, no. 5, pp. 1044–1054, May 2014.
- [23] K.-W. Lao, N. Yi Dai, W. Liu, M.-C. Wong, and C.-K. Wong, "Modeling and control of railway static power conditioner compensation based on power quality standards" in *Proc. IEEE 13th Worksh. Control Modeling Power Electron.*, 2012, pp. 1–6.
- [24] K. W. Lao, N. Dai, W. G. Liu, and M. C. Wong, "Hybrid power quality compensator with minimum dc operation voltage design for high-speed traction power systems," *IEEE Trans Power Electron.*, vol. 28, no. 4, pp. 2024–2036, 2013.
- [25] K. W. Lao, M. C. Wong, N. Y. Dai, C. K. Wong, and C.-S. Lam, "A systematic approach to hybrid railway power conditioner design with harmonic compensation for high-speed railway," *IEEE Trans. Ind. Electron.*, vol. 62, no. 2, pp. 930–942, Feb. 2015.
- [26] K. W. Lao, M. C. Wong, N. Dai, C. K. Wong, and C.-S. Lam, "Analysis of DC link operation voltage of a hybrid railway power quality conditioner and its pq compensation capability in high speed co-phase traction power supply," *IEEE Trans. Power Electron.*, vol. 31, no. 2, pp. 1643–1656, Feb. 2015.
- [27] Y. Kunshan, *Electric Railway Power Supply and Power Quality*. China Electric Power Press, 2010.
- [28] C. S. Lam, M. C. Wong, and Y.-D. Han, "Hysteresis current control of hybrid active power filters," *Power Electron. IET*, vol. 5, no. 7, pp. 1175–1187, Aug. 2012.
- [29] Ma, M. Wu, and S. Yang, "The application of SVC for the power quality control of electric railways," in *Proc. Int. Conf. Sustainable Power Gener. Supply*, 2009, pp. 1–5.



**Keng-Weng Lao** (S'09) was born in Macau, China, in 1987. He received the B.Sc. and M.Sc. degrees in the electrical and electronics engineering in 2009 and 2011, respectively, from the Faculty of Science and Technology, University of Macau, Macao, China, where he is currently working toward the Ph.D. degree from the Department of Electrical and Computer Engineering.

His current research interests include FACTS compensation devices, energy saving, and renewable energy.

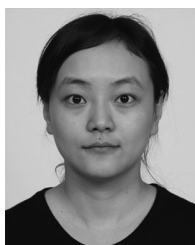
Mr. Lao was the recipient of first runner-up of the Challenge Cup National Interscience and Technology Competition, and Championship of the Postgraduate Section in the IET Young Professionals Exhibition and Competition in China and Hong Kong, respectively, in 2013. He was also the recipient of the Champion Award of the Schneider Electric Energy Efficiency Cup in Hong Kong in 2010.



**Man-Chung Wong** (S'98–A'03–M'04–SM'06) received the B.Sc. and M.Sc. degrees in electrical and electronics engineering from the Faculty of Science and Technology, University of Macau, Macao, China, in 1993 and 1997, respectively, and the Ph.D. degree from the Tsinghua University, Beijing, China, in 2003.

He has been an Associate Professor at the University of Macau since 2008. His current research interests are FACTS and DFACTS, power quality, custom power and PWM.

Dr. Wong received the Young Scientist Award from the "Instituto Internacional De Macau" in 2000, the Young Scholar Award from the University of Macau in 2001, the second prize of 2003 Tsinghua University Excellent Ph.D. thesis award, and the third prize of 2012 Macao Technology Invention Award given by Macao Science and Technology Fund (FDCT).



**Ning Yi Dai** (S'05–M'08–SM'15) received the B.Sc. degree in electrical engineering from the Southeast University, Nanjing, China, in 2001, and the M.Sc. and Ph.D. degrees in electrical and electronics engineering from the Faculty of Science and Technology, University of Macau, Macao, China, in 2004 and 2007, respectively.

She is currently an Assistant Professor in the Department of Electrical and Computer Engineering, University of Macau. She has published more than 60 technical journals and conference papers in the

field of power system and power electronics. Her research interests include application of power electronics in power system, renewable energy integration, and pulse width modulation. She was the co-recipient of the Macao Science and Technology Invention Award (Third-Class) in 2012.



**Chi-Seng Lam** (S'04–M'12–SM'16) received the B.Sc., M.Sc., and Ph.D. degrees in electrical and electronics engineering from the University of Macau (UM), Macao, China, in 2003, 2006, and 2012 respectively. In 2009, he simultaneously worked as a Laboratory Technician and started to pursue the Ph.D. degree, and completed Ph.D. within 3 years.

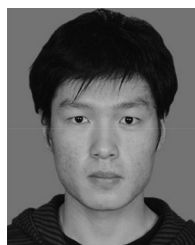
From 2006 to 2009, he was an E&M Engineer in UM. In 2013, he was a Postdoctoral Fellow in The Hong Kong Polytechnic University, Hong Kong, China. He is currently an Assistant Professor in the State Key Laboratory of Analog and Mixed-Signal VLSI, UM. He has co-authored 2 books: *Design and Control of Hybrid Active Power Filters* (Springer, 2014) and *Parallel Power Electronics Filters in Three-phase Four-wire Systems - Principle, Control and Design* (Springer, in press), 1 U.S. patent, 2 Chinese patents, and more than 50 technical journals and conference papers. His research interests include integrated power electronics controllers, power management integrated circuits, power quality compensators, smart grid technology, renewable energy, etc.

Dr. Lam received Macao Science and Technology Invention Award (Third-Class) and R&D Award for Postgraduates (Ph.D.) in 2014 and 2012, respectively. He also received Macao Government Ph.D. Research Scholarship in 2009–2012, Macao Foundation Postgraduate Research Scholarship in 2003–2005, the 3rd RIUPEEEC Merit Paper Award in 2005. In 2007, 2008, and 2015, he was the GOLD Officer, Student Branch Officer and Secretary of IEEE Macau Section. He is currently the Vice-Chair of IEEE Macau Section and Secretary of IEEE Macau PES/PELS Joint Chapter. He was the Local Arrangement Chair of TENCON 2015 and ASP-DAC 2016.



**Chi-Kong Wong** (M'91) was born in Macao, in 1968. He received the B.Sc. and M.Sc. degrees in electrical and electronics engineering (EEE) from the University of Macau, Macao, China, in 1993 and 1997, respectively, and the Ph.D. degree in EEE from Tsinghua University, Beijing, China, in 2007.

He was recruited by the University of Macau as a Teaching Assistant for the Faculty of Science and Technology in 1993 and promoted to the post of Lecturer and Assistant Professor in 1997 and 2008, respectively. Since 1997, he has been teaching the fundamental courses in the Department of Electrical and Electronics Engineering and supervising the final year projects. In addition of the undergraduate teaching and supervision, he had also co-taught one master course and co-supervised three master research projects. His current research interests include voltage stability analysis, synchronized phasor measurement applications in power systems, wavelet transformation applications in power systems, renewable energy, and energy saving. From 1997 to 2007, he had conducted four university research projects and five external projects form CEM and organized one power system protection training course to CEM staff.



**Lei Wang** received the B.Sc. degree in electrical and electronics engineering from the University of Macau (UM), Macao, China, in 2011, and the M.Sc. degree in electronics engineering from Hong Kong University of Science and Technology (HKUST), Hong Kong, in 2012. He is currently working toward the Ph.D. degree in electrical and computer engineering from the Power Electronics Laboratory, UM.

His current research interests include power electronics, power quality and distribution flexible AC transmission system (DFACTS), power quality compensation, and renewable energy.

Mr. Wang received the champion award in the "Schneider Electric Energy Efficiency Cup," Hong Kong, 2011.